A novel powder-epoxy towpregging line for wind and tidal turbine blades

A novel powder-epoxy towpregging line for wind and tidal turbine blades

Colin Robert*, Toa Pecur, James M. Maguire,

Austin D. Lafferty, Edward D. McCarthy, Conchúr M. Ó Brádaigh

School of Engineering, Institute for Materials and Processes, The University of Edinburgh, Sanderson Building, King's Buildings, Edinburgh, EH9 3FB, UK

*Corresponding author

Keywords: Powder-epoxy, towpregging, joule heating, carbon fibres, basalt fibres, hygrothermal ageing

Highlights:

- The powder-epoxy towpregging process was described in detail for both carbon fibres and basalt fibres.

- Excellent static mechanical properties were reported for unidirectional carbon-fibre/powder-epoxy composites and the influence of fibre volume fraction (FVF) was analysed.

- Two types of basalt fibre were tested, showing comparable mechanical properties to glass fibre composites.

- A hygrothermal study of both carbon-fibre composites and basalt-fibre composites showed that the latter had a greater sensitivity to water uptake and immersed ageing.

Abstract

A novel material and process was developed using fibre-reinforced powder-epoxy to produce unidirectional towpreg with a pilot-scale towpregging line, for cost-effective production of large composite structures for the renewable energy market, specifically for wind and tidal turbine blades. Electrostatic attraction was used to coat fibre tows with powder epoxy and either joule or radiant heating employed to heat and melt the polymer, followed by consolidation between rollers. Unidirectional carbon-fibre and basalt-fibre reinforced polymer laminates (UD-CFRP and UD-BFRP, respectively) were manufactured from the towpreg. Tensile test results showed that the towpregging process could be employed to achieve high performance UD-CFRP with 0° tensile properties that are similar or better than commercially-available UD-CFRP systems. The competitive advantages of the powder-epoxy towpreg system include lower cost, better overall manufacturing control for vacuum-bag-only manufacturing and the ability to co-cure parts together at a later stage. Mechanical test results showed some variation between two types of UD-BFRP, but the results compared well with published data on UD-BFRP and equivalent glass-fibre reinforced polymer (GFRP) systems. Finally, the influence of hygrothermal ageing due to water immersion on the tensile properties of the materials was investigated, with tests revealing that the water ageing effect was more severe in the case of UD-BFRP than for UD-CFRP.

1. Introduction

The International Energy Agency has reported an increasing rate of electricity generation worldwide of 8.28% per year over the last 50 years [1], which has been accelerating in the last two decades to sustain emerging economies. Despite a rapid expansion of renewable energy sources in the past 20 years [2], the overall contribution of renewable energy is still modest (1.8% for wind and solar, 2.5% for hydro) in comparison to global energy consumption. In this regard, optimisation and diversification of renewable energy sources and technologies have become paramount. Ocean energy potential, although very substantial at an estimated 8,000 TWh/year [3], is still largely under-exploited.

To exploit the full potential of offshore energy, in particular, several significant challenges must be addressed for wind and tidal turbine composite structures. These structures operate in severe environments undergoing high fatigue loading, water ingress, erosion, immersed ageing, bio-fouling, etc. [4–8]. Accordingly, the composite structures must have high mechanical properties, which cannot degrade significantly over the lifespan of the device (approx. 20 – 25 years). GFRP has been used predominantly in the manufacture of wind and tidal turbine blades due to its good mechanical performance, relatively low cost, and formability for complex geometries. As these blades get larger, however, the demand on mechanical performance increases, along with the need to lower the levelised cost of energy (LCOE).

For several years, basalt fibres have been investigated as a potential alternative to glass fibres; in particular, for E-glass fibres, which are widely used by the composites industry [9,10]. Basalt fibres are reported to have similar mechanical properties to S-glass fibres, however, the basalt fibre production requires less energy and less additives than glass fibre production [11], meaning that it costs less than S-glass [10]. In general, it has been shown in the literature that BFRP has mechanical properties which are comparable to, if not higher than, GFRP [11,12]; albeit, with considerable variation in reported properties. Some of this variation may be linked to basalt being from a natural source with a chemical composition that depends on location, as well as the typical variations between suppliers ascribed to their production methods [10]. In this regard, BFRP has not had the same level of evaluation as GFRP and CFRP to build a comprehensive knowledge of its mechanical behaviour. In the context of this paper, there are few studies which have documented the immersed performance of BFRP for marine applications [13–15]. Nevertheless, basalt fibre technology continues to advance, and the aforementioned studies reported sufficiently promising results to warrant further investigation as a potential alternative to GFRP for wind and tidal turbine blade manufacture.

Where higher performance materials are required, CFRP has also been investigated as an alternative to GFRP due to its high specific strength and stiffness. To maintain a low LCOE, however, careful consideration of blade design is required to optimise the cost effectiveness of introducing CFRP [16]. Many wind turbine blade manufacturers have implemented hybrid composite designs to offset the associated costs [4,6,17–21] (e.g. a CFRP spar with a GFRP root, shear web, and skins). As the main load bearing sub-structure along the span of the blade, the spar must withstand significant tensile and compressive stresses. Consequently, spars are very thick unidirectional laminates. Depending on the blade size and design, the spar may taper from 150 mm thickness down to less than 5 mm [6,22]. For wind turbines, this occurs over a larger span (e.g. 70 m) than for tidal turbine blades (e.g. 8.5 m). The spar caps for a 2 MW tidal turbine blade can taper from 104 mm thickness to 25 mm [23].Manufacturing such laminates poses several processing challenges including maintaining fibre alignment and straightness [24], difficulty infusing with conventional methods (such as vacuum-assisted resin transfer moulding (VaRTM)) [6], and difficulty in controlling the exothermic curing reaction of the resin matrix [25]. Accordingly, several material suppliers have developed UD-CFRP vacuum-bag-only (VBO) prepregs specifically aimed at manufacturing spars and similar structures for

wind and tidal turbine blades; Gurit's SparPreg™, Hexcel's Hexply M9.6 series and M79 prepreg, and Cytec's (formerly ACG's) VTM 260 series [4]. The advantages of these VBO prepregs is that they greatly reduce the complexity of the infusion process as they are supplied in a partially or fully impregnated form. Their disadvantage is that they typically require temperature-controlled storage to prevent premature curing of the resin system (i.e. out-time effects [26]), and they generally do not address the issue of high exotherms, with the exception of Hexcel's Hexply M79 resin [27]. One alternative that allows blade manufacturers to avoid infusing dry fabric and controlling large exotherms, is the use of pultruded UD-CFRP [18,20,28], which has even been considered for offshore wind turbine tower structures [29]. Pultruded sections are fully infused (usually to a relatively high fibre volume fraction) and they are typically pre-cured, so they have no exotherm, they don't require temperature-controlled storage, and their high degree of fibre alignment is "locked in". The major disadvantage with these fully-cured pultruded sections is that they are difficult to form to complex geometries, such as the double curvatures in turbine blades, and they must be adhesively bonded together to form a single spar.

The technology described in this paper aims to address the aforementioned disadvantages of conventional VBO prepregs and pultruded sections by utilising the unique properties of a novel powder-epoxy matrix. In relation to fibre-reinforced composites, this powder-epoxy has been the subject of several studies in recent years which have investigated its processing behaviour [30–32], its mechanical behaviour [33–35], its behaviour in immersed conditions [36], and its application in wind [17] and tidal turbine blades [23,37]. Powder-epoxies, along with other thermosetting powders, are a commodity product from the coatings industry, which are widely available in bulk from a range of suppliers (e.g. FreiLacke, DSM, AkzoNobel, 3M, etc.). These powders tend to have excellent storage stability due to a high initial glass transition temperature (around 40°C) [38] and the frequent use of heat-activated latent curing agents in their formulation [39]. This means they can be used to make VBO prepregs which do not require temperature-controlled storage and generate significantly less exotherm than conventional epoxy systems [30,32]. Moreover, due to the processing stability of the powder-epoxy [30], it has been shown that sub-components (e.g. turbine blade skins) can be infused at 120°C, cooled to ambient conditions to form solid β-staged preforms (i.e. partially cured), assembled together, and then co-cured at 180°C [40]. The ability to store powder-epoxy preforms for use at a later stage is a strong competitive advantage of this technology. The ability to then co-cure these pre-formed parts is also very interesting, especially for the wind industry where blades are usually manufactured in sections and then adhesively bonded. The new process can thus avoid an extra processing step while maintaining the mechanical properties at the joining line, which can sometimes be design-critical.

The powder-epoxy is used in this study for the production of 'towpreg' a.k.a. pre-impregnated tows. In short, this production process consists of spreading the fibres of a tow, depositing powder between the fibres, heating the coated fibres, and then consolidating them. Spanning the last four decades, towpregging has been investigated by several authors for both thermoplastics and thermosets [41–45]. It has been shown that this production route has benefits over hot melt prepregging and solution prepregging in terms of cost and environmental impact; including little or no volatile organic compounds (VOCs) and little waste disposal due to powder reclamation and reuse [46]. Towpreg can be used for automated tape placement (ATP); either as a single towpreg (a.k.a. automated fibre placement (AFP)) or several consolidated towpreg (a.k.a. automated tape laying (ATL)) [44,47]. It can also be used in pultrusion [42,48] or filament winding [45]. This versatility lends itself to many industrial applications, however, to the authors knowledge there is little or no evidence to suggest it has been applied to the production of wind or tidal turbine blades or structures.

Initial work has been carried out on developing a pilot-scale powder towpregging for the aforementioned application [49,50]. In this study, a more mature version of the pilot powder towpregging line is described. Both carbon-fibre towpreg and basalt-fibre towpreg are investigated as alternatives to GFRP systems. Mechanical testing is carried out on UD-CFRP laminates made from the CF towpreg and compared with existing data to determine if the towpregging process has an adverse effect on the mechanical performance of the carbon fibres. The influence of fibre volume fraction, and its variability with respect to the towpregging line, is also studied for carbon-fibre towpreg. UD-BFRP laminates are made using basalt fibres from two different suppliers. These laminates are mechanically tested to study the variation between suppliers. Mechanical results for UD-BFRP are also compared with published data on equivalent material systems. Finally, a hygrothermal ageing study is carried out on UD-CFRP and UD-BFRP to assess the performance of both materials in immersed conditions.

2. Materials

2.1. Terminology

In the literature relating to material development and material production, the term 'towpreg' has been used commonly to describe tows that are impregnated with a thermoset powder or a thermoplastic powder [44,51,52]. For clarity, in this work, 'tow' is used to refer to the unimpregnated tow, and 'towpreg' is used for one or more tows that have been impregnated with powder and then sintered and consolidated, but which are still uncured. This terminology is chosen because 'towpreg' represents a highly versatile precursor material which can later be developed for numerous manufacturing processes including pultrusion, ATP, filament winding, etc.

2.2. Powder-epoxy

All the composites in this study were manufactured using a novel powder-based epoxy matrix. The powder-epoxy (PE6405, density 1220 kg/m^3) was engineered by Swiss CMT and then produced by FreiLacke. The processing characteristics of the powder-epoxy can be defined by two steps, which are relevant to both towpreg production and laminate manufacturing:

a) The powder-epoxy melts and sinters at around 40-60°C, reaching a minimum viscosity for infusion around 120°C.
b) The curing is then carried out through a heat activated catalytic process where the curing agent requires a temperature of at least 145°C for reaction initiation, as described by Maguire et al. [30] and Mamalis et al. [33] and shown by differential scanning calorimetry (DSC) in Figure 2.

The details of the chemistry involved are proprietary to the manufacturers of these commercially available products. The powder-epoxy has numerous advantages compared to standard VBO prepreg systems when building large, thick -section structures such as the latest wind turbine blades (over 100 mm thickness at the blade root). Firstly, the low melt viscosity (minimum of 1.26 Pa.s [30]) and low rate of cure below 120°C allows more time to fully infuse the section [30–32]. Secondly, as shown in Figure 1, the powder-epoxy, PE6405 displays a curing exotherm of approx. 140 J/g, which is less than a third of the enthalpy of standard liquid resin epoxy systems (about 500 J/g) [30]. This feature is crucial in reducing the risk of thermal runaway for thick section composites manufacturing which allows for quicker production rates [31,32].

Figure 2 also highlights the powder-epoxy's ability to separate the melting/sintering phase (ending at 80°C) from the curing phase (starting at 145°C). Since the PE6405 melting/sintering temperature is considerably lower than the curing temperatures, composite parts can be impregnated in one stage, and then cured in another. For this reason, a two-stage heating profile is typically used as presented in Figure 2. As previously mentioned, this feature gives manufacturers the ability to reform and co-cure complicated parts as necessary. This strongly increases the cohesion of the different parts and removes the need for an extra adhesion step, thus allowing 'one-shot' manufacturing, as shown in Figure 3 [40,53,54].

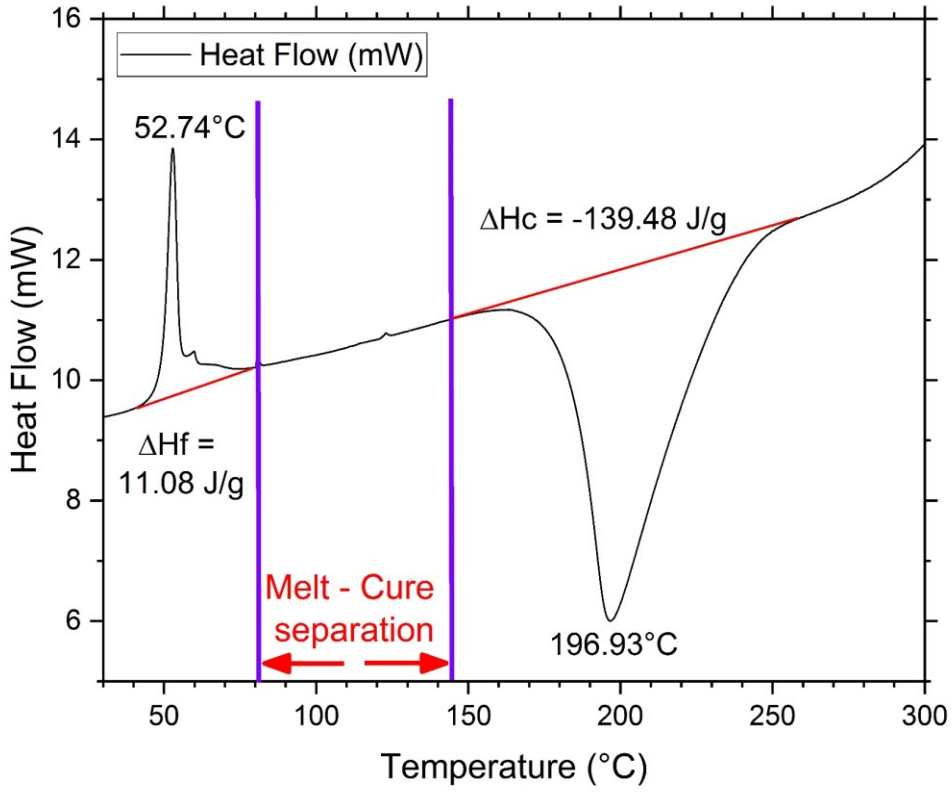

Figure 1: DSC data showing a temperature sweep (20°C/min) of neat powder-epoxy sample, exhibiting peaks due to a reversal of enthalpic relaxation (at 52.74°C) and curing (at 196.93°C). The temperature gap between the end of the melting/sintering and the beginning of the cure is represented by the purple lines. Note: exotherm is downwards.

In recent times, 'one-shot' manufacturing processes have been targeted by both the wind and tidal energy industries due to the added cost and weight of adhesives, as well as the potential for adhesive bondlines to act as 'weak spots' in the structure [5,55]. These reported technologies all utilise some form of VaRTM process to manufacture their 'one-shot' structures, but as Harper et al. [5] acknowledge, it is unclear whether such processes can be used to successfully thick sections in 'one-shot' (due to exotherms and difficulty infusing), or whether thick-section parts must be prefabricated and later introduced during infusion of the skins [55]. In contrast, the low-exotherm powder-epoxy 'one-shot' technology can be used with VBO prepreg materials, thus reducing the risk of poor infusion or 'thermal runaway'.

One limitation to the powder-epoxy technology is that the heat-activated curing agent requires higher temperatures for curing (> 160°C) than what is typical for conventional processes like VaRTM. Nevertheless, integrally-heated ceramic tooling has been developed to achieve the required processing conditions, and was used to produce "one-shot" 12.6m wind turbine blades, shown in Figure 3, using glass-fibre/powder-epoxy VBO prepregs [40].

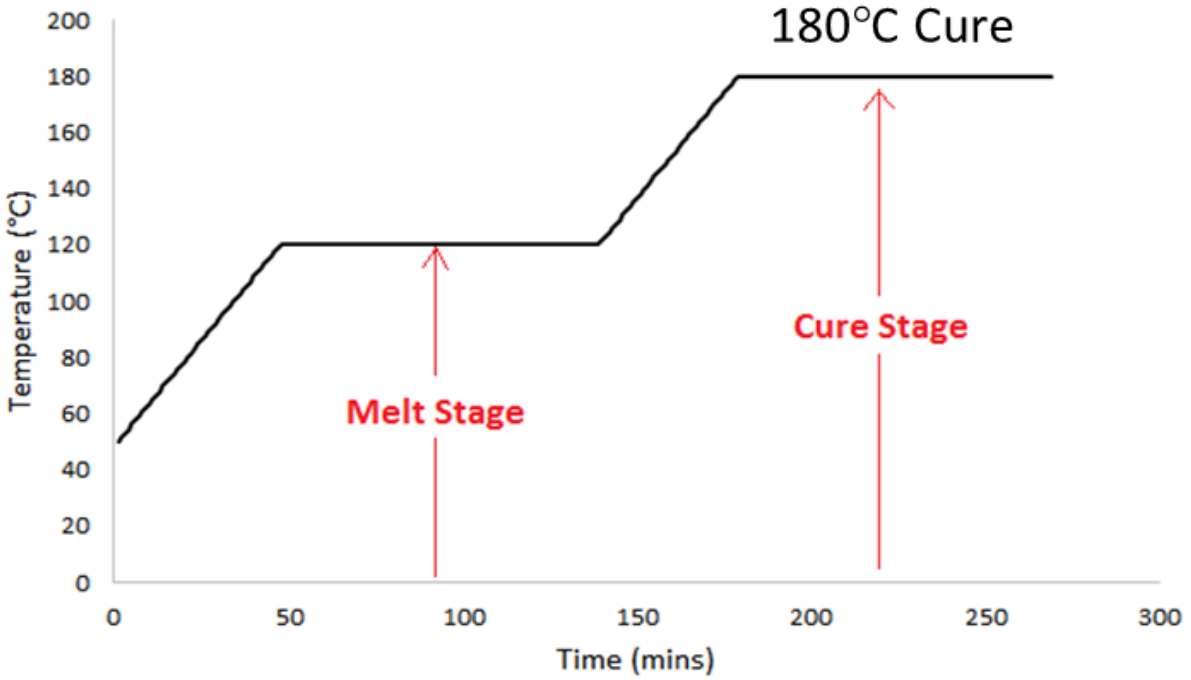

Figure 2: Typical melting and cure cycle for processing of powder-epoxy composites. Powder-epoxy composites can be melted and consolidated at 110-120°C without any significant curing, thus allowing individual components to be consolidated and assembled for a final co-cure at 180°C.

Figure 3: Ceramic heated tools (left); and 12.6 m blades made from powder-epoxy based VBO prepreg (right) [39]

2.3. Carbon fibres

Mamalis et al. investigated the influence of sizing and fibre straightness on the mechanical properties of PE6405 powder-epoxy reinforced with Toray T700S-24K carbon fibres (CF) [33,35]. In their studies,

it was found that fibre straightness had a significant effect on mechanical properties, and the 50C sized CF were found to be superior compared to two other fibre sizings. As such, T700S-24K-50C fibres (equivalent to 1650 Tex) from Toray Industries Inc. [56] were chosen for this study; with individual fibres having a diameter of 11 µm.

2.4. Basalt fibres

Variation in basalt fibre (BF) quality between different suppliers is common, as basalt is naturally sourced from volcanic rocks, producing different chemical compositions when forming [11]. The precise details of fibre manufacturing and sizing processes are often kept confidential, which leads to greater uncertainty on the quality and reproducibility of the fibres. To address these concerns, the properties of two different commercially available basalt fibres were investigated and compared in this study; BF from Basaltex [57,58], and BF from Mafic [59]. Both Mafic BF and Basaltex BF had a fibre diameter of 13 µm, and were supplied in the form of 2400 Tex assembled rovings. The fibres were both coated in alkoxysilane sizing, usually used in glass fibres for optimal cohesion with epoxide systems [58,59]. A comprehensive summary of fibres and matrix mechanical properties are presented in the table below.

Table 1: Individual mechanical properties of fibres and powder epoxy matrix

	σ_M (MPa)	E (GPa)	ε_f (MPa)	Diameter (µm)	Density (g/cm^3)
T700s carbon fibres [56]	4900	230	2.1	7	1.81
Mafic© direct roving [59]	3100	88-92	3.5	13	2.63
Basaltex© direct roving [58]	2900-3100	85-89	3.5	13	2.67
PE6405 from Freilacke© [35]	73.1	3.0	2.43*	N/A	1.22

** linear elastic behaviour assumed*

3. Towpregging process

3.1. General description of the towpregging line

The pilot towpregging line was designed and constructed based on existing designs from the literature, such as the thermoplastic towpregging developed by Edie et al. [41]. Figure 4 represents the different steps of the process; all of which have an effect on the final properties of the towpreg. These steps are briefly described below to give a general understanding of the towpregging line, prior to going into further detail in the next sections.

a) The tows were guided through steel rings and tensioned with two interlocked Polytetrafluoroethylene (PTFE) rollers.
b) Extra tension was applied using two additional PTFE rollers and the tows were merged by a chamfered roller.
c) The fibres were pulled through the deposition chamber where an electrostatic spray gun deposited powder particles onto the fibres at a 90° angle.
d) Heat was applied to the powder-coated fibres via an energy source tailored to the fibre type in order to melt the powder.
e) The towpreg was cooled in ambient air under tension.
f) Finally, the vitreous towpreg was wound-up on a drum, which was motorised to keep the whole line under tension.

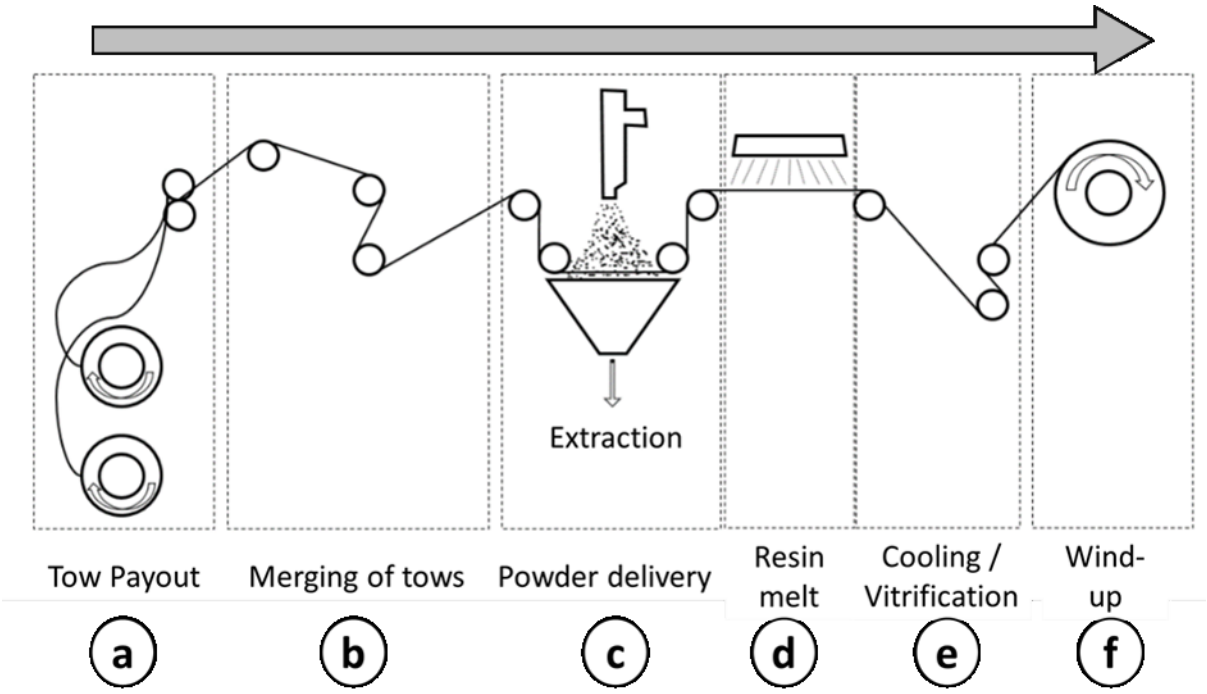

Figure 4: Towpregging line schematic. The arrow indicates the direction in which the tow is travelling.

3.2. Tow payout

Tow payout for this study involved two tows being unwound from the as-supplied material drum while under tension. The payout design included grooves to guide the tensioning belts, a tapered internal cap diameter which could work with different drum sizes, and a ball bearing system for smoother tow payout. This system provided stable tension, which allowed for homogenised merging of the two tows on a grooved PTFE roller.

3.3. Powder deposition

There are numerous methods of powder deposition for the towpregging process. Several of these methods were reviewed by Padaki and Drzal [60] including four types of fluidised bed deposition, powder slurry deposition, and electrostatic spraying. Another method is ‘powder curtain’ deposition which uses an auger to disperse powder across the tow as it passes underneath [44,61]. Early

iterations of the pilot towpregging line (presented herein) implemented a form of 'powder curtain' deposition; using a vibrating hopper and mesh to create the 'powder curtain' [62]. This method, however, resulted in inconsistent powder dispersion along the towpreg.

For this study, electrostatic spraying was chosen as the method of powder deposition. A 60 W Encore LT electrostatic spray gun, from Nordson, was used to coat the fibres within an enclosed acrylic spray box (Figure 5). The gun was set to 100 kV at 60 µA, using the smart flow setting for both the air and the powder flows, which helped with adjusting the flow to maintain the same powder velocity. The pressure was set to 5 bar. The surplus powder was evacuated from the spray box using a Nilfisk VHS-110 ATEX extraction unit with High Efficiency Particulate Air HEPA filter (1.1 kW), kept at maximal flow throughout the process to avoid clogging. The powder was recycled to avoid any waste.

The electrostatic attraction between the powder-epoxy and the tows was due to the powder being negatively charged by a corona electrode as it passed through the spray gun, while the tows were grounded. This phenomenon has been modelled for towpregging by Woolard and Ramani [63]. They demonstrated that electrostatic spray can coat both sides of the tow due to a 'wrap-around' effect, but that the strength of this effect was dependent on the spread tow width. Tow width was constant during this study so as not to introduce variability in powder deposition. This was achieved using grooved rollers at various points in the line.

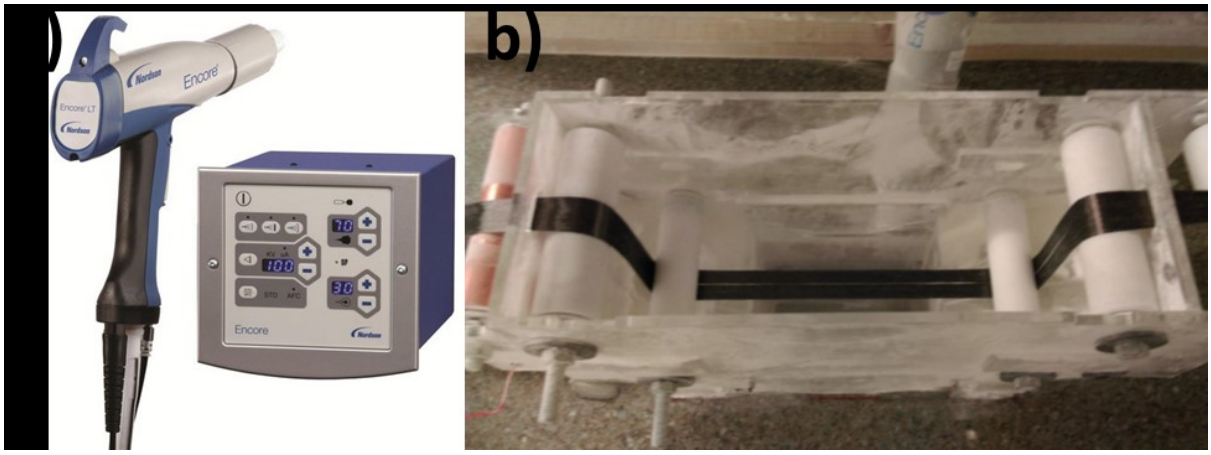

Figure 5: a) Encore LT electrostatic spray gun and its control board (© Nordson). b) Plan view of the spray box where a cloud of negatively charged powder-epoxy coats the merged tows.

3.4. Electrical heating of carbon fibre towpreg

As carbon fibres are electrically conductive, it has been shown by others that passing a direct current (DC) through the fibres can be used to heat towpreg [41,64] or even cure composite structures [65]. This resistive heating is due to the Joule effect, and can achieve rapid increases in temperature while requiring less energy than conventional heating methods [65]. For this reason, resistive heating technology was employed in this study when producing CF towpreg. As shown in Figure 6, two copper rollers were connected to a DC generator using carbon brushes and a differential of 12 volts was set. As the CF passed between the rollers, they closed the circuit and generated heat. The current drawn oscillated between 140 and 160 mA, for a power consumption of only 1.68W to 1.92W. The current fluctuation was due to contact resistances, because of changes in both tow tension and powder concentration during processing.

The temperature was monitored with an FLIR TG54 Spot IR Thermometer and was controlled to reach 120°C. The powder in contact with the fibres melted rapidly (Figure 6), demonstrating the ability to work at high speed (up to 15 metres per minute for a 50% fibre volume fraction), while keeping a constant temperature profile between the copper rolls. The copper rollers were coated with a release agent (Frekote 55-NC) and cleaned after each use to avoid any contaminants and inhomogeneity due to excess resin. The first two metres of towpreg were discarded for each run because, at start up, the towpregging line required some time to reach steady state conditions. Removing the first two metres also reduced the risk of any contamination due to Frekote residue.

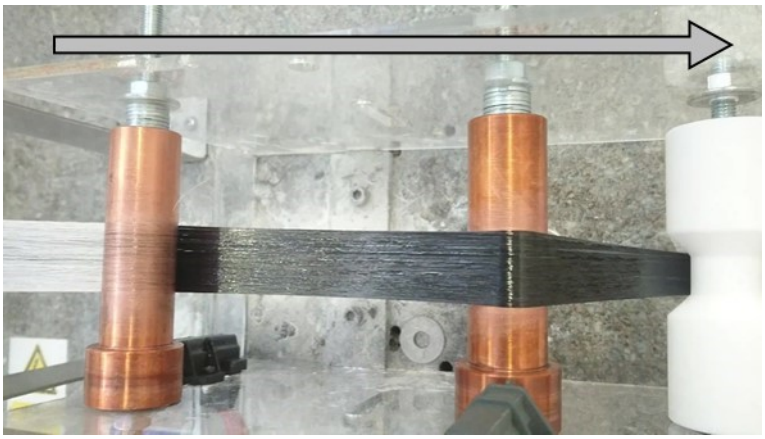

Figure 6: DC electrical heating using copper rollers (plan view). The powder-epoxy coated tows (white) approach the first copper roller on the left. As the tows pass between the rollers, the powder-epoxy melts and sinters onto the carbon fibres (black). The arrow indicates the direction in which the tow is travelling.

3.5. Infrared heating for basalt fibre towpreg

Due to basalt fibres (BF) being non-conductive, an alternative heat source was required for processing the BF towpreg. From the literature, possible alternatives included tunnel ovens [66–68], convection ovens [41,69,70], hot gas torches [67,69], infrared lamps [61,68,70], and microwave ovens [41]. In this study, the towpregging line used a 1kW infrared (IR) lamp. This lamp had an adjustable power, was 30 cm long, and had a reflector to focus radiated heat towards the substrate surface. Again, the temperature was monitored using an IR thermometer throughout the process. To maintain a homogenous heating profile, the maximum line operating speed was set at 5 m/min. The temperatures, however, were initially found to be lower on the non-exposed side. As such, an additional reflective system (a copper sheet) was added to improve the temperature homogeneity on both sides of the BF tow.

3.6. Cooling and recovery

After the powder was melted, the towpreg proceeded to a grooved roller to maintain a constant width. It was then cooled quickly (in about five seconds) by convection and radiation to the surrounding atmosphere, prior to being wound up onto the winding drum. The towpreg temperature, located immediately before the winding drum, was consistently between 30°C and 40 °C, which was

lower than the melt temperature of the epoxy. Hence, the towpreg was wound in a vitreous state and maintained optimal straightness due to the tension applied to the fibres throughout the process. The rotating drum itself was powered by a Mellor electric 24 V DC Brushed DC Geared Motor with a maximum output speed of 5.3 rpm. As the drum itself had a diameter of 40 cm, the maximum towpregging process speed was 6.66 m/min. As the processing speed wasn't a constraint in this study, the motor speed was the main parameter used in order to control the fibre volume fraction (FVF) of the towpreg. In this study, all towpreg samples were manufactured using the same powder-epoxy (PE6405).

4. Composite plate manufacturing and testing

4.1. Manufacturing overview

The overall manufacturing system, illustrated in Figure 7, is described briefly below. Further details are given in subsequent sections.

Stages 1 – 2: Towpreg was produced on the towpregging line.

Stages 2 – 3: The towpreg was cut into strips of exactly 30 cm length using a guillotine system.

Stages 3 – 4: The towpreg strips were aligned and clamped in the fibre tensioning apparatus. This is used to ensure tow straightness in the unidirectional plates during cure.

Stages 4 – 5: The tensioned preform was cured under vacuum to produce a unidirectional composite plate.

Stages 5 – 6: The composite plate was tabbed and cut, and the resulting specimens were tested and characterised.

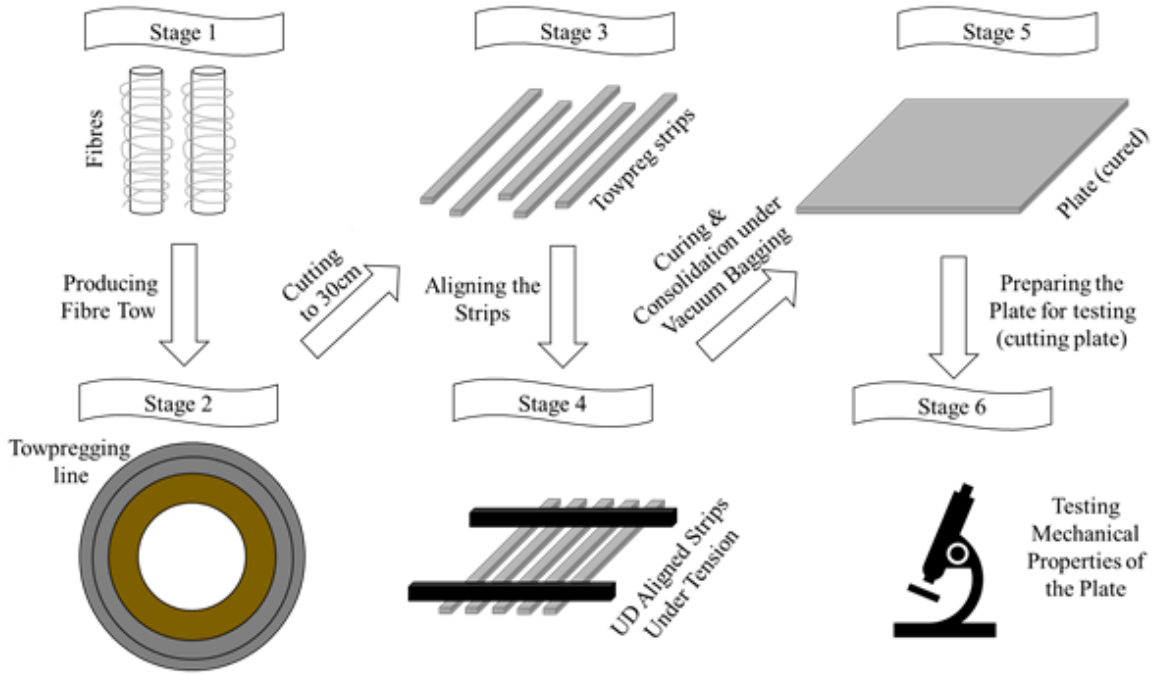

Figure 7: Manufacturing overview - from tows to plate manufacturing and testing.

4.2. Plate manufacturing

It has been shown that fibre misalignment and fibre 'waviness' can affect the mechanical performance of FRPs [24,71,72]. The results presented by Mamalis et al. [33,35] confirmed that tensioning unidirectional CF/powder-epoxy improved the mechanical properties of the material by increasing the fibre straightness and alignment. Using the towpregging line, highly aligned CF/powder-epoxy may be realised through automation, however, additional handling and processing of tows can lead to increased fibre breakage [43,44]. Therefore, the composite plates for this study were manufactured using the same tow tensioning apparatus developed by Mamalis et al. [33] so that a direct comparison could be made between the two sets of results. By comparing the two, it would be possible to determine if the towpregging process caused any significant fibre damage or breakage.

For the plate manufacturing, 30 cm long towpreg 'strips' were cut and placed on a PTFE coated flat steel plate; alignment was aided using a plastic grid (see Figure 8a). Once all the strips were placed correctly, they were locked in place by the tensioning apparatus (described further in [33]). Five layers of strips were necessary to obtain 1 mm thick plates. After the alignment grid was removed, a tensioning force of approx. 3.0 kN was applied. This was the force chosen by Mamalis et al. [33], to achieve optimal alignment of the T700S-24K-50C tows. An extra PTFE coated plate was placed on the top of the tensioned towpreg, and the whole tensioning apparatus was then vacuum bagged. The system was kept under vacuum at all times during processing. The curing cycle was set at 40 °C for 12 hours to remove all form of moisture from the strips. The temperature then ramped to 130°C for 2 hours, melting the powder and consolidating the system. Following this, the plate was cured at 185°C for 2 hours and then cooled to ambient temperature. This methodology was used to produce both UD-CFRP and UD-BFRP plates.

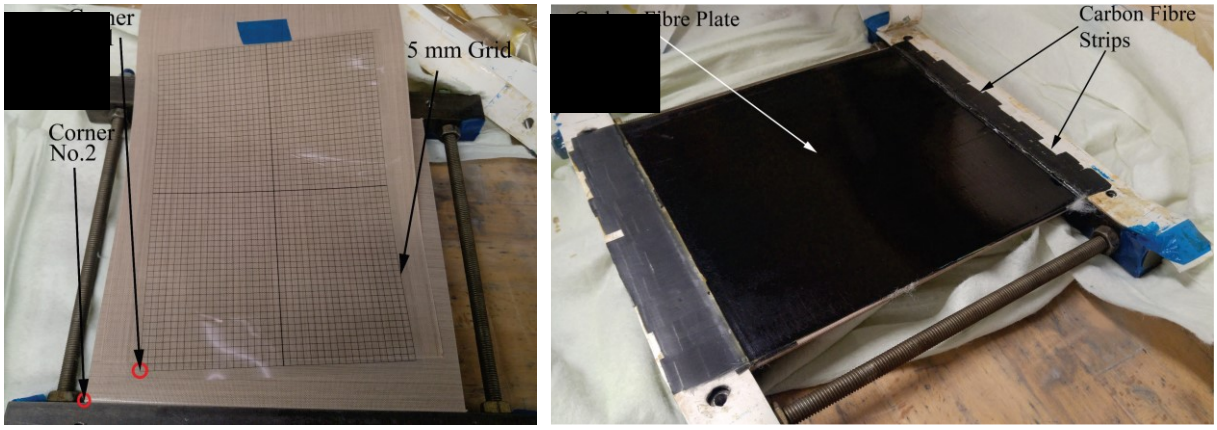

Figure 8: Tensioning rig system: a) Strip alignment using a grid, b) Cured plate.

4.3. Quality control - weight measurements and void analysis

Fibre volume fraction has an important influence on the mechanical properties of the composite materials. As powder deposition may vary during towpreg production [61], it was important to understand what influence this may have on the mechanical properties of the cured laminates. Different FVF towpreg were produced by slightly modifying the line speed. For each line speed setting, 30 cm strips of towpreg were cut and weighed, and the FVF of each strip was determined based on the known volume and mass of the virgin fibre tows. Resin burn-off was also performed on random samples to cross-check their FVF; ASTM D3171-15 – Procedure G – kept at 550°C for 60 min in high temperature furnace.

To investigate the influence of FVF over a wide range, the strips were filtered according to four FVF sub-groups: 45% to 50%, 50% to 55%, 55% to 60% and 60% to 65%. A plate for each FVF sub-group was manufactured using the methodology described in the previous section.

Optical microscopy was also used in this study. A UD-CFRP specimen was cut into 10 samples and embedded in epoxy. The 10 embedded samples were polished, and their cross sections were observed using an Axioskop® 2MAT optical microscope (Figure 9a). 50 photos (5 per sample) were taken with Axio vision SE64® software, and a FVF analysis was performed on ImageJ®, with 8 bits grayscale settings (Figure 9b). Two filters were used to differentiate the resin, fibres and porosity (fibres contrast threshold: 117 to 255, voids contrast threshold: 0 to 14). The fibre to resin to void surface ratio obtained on each individual photos, combined with a large set of 50 samples, allowed for a FVF estimate. This quantitative method allowed not only to crosscheck the FVF, but also to detect and determine the sample's porosity, as shown in Table 2. The table displays a low porosity (0.437%) compared to other VBO systems and tapes [73]. It is worth noticing that the FVF was found slightly below target (52.07% instead of 52.50%).

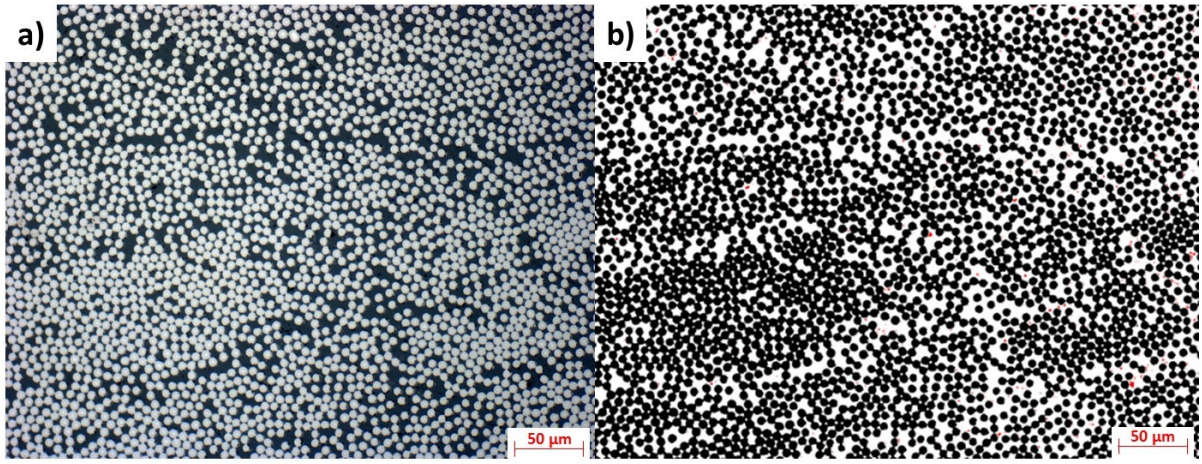

Figure 9: a) Optical microscopy of a powder-epoxy UD-CFRP cross section in reflection mode. b) Resin (white), fibres (black), and voids (red) identified using volume fraction analysis with ImageJ software filters.

Table 2: Quantitative study of porosity and FVF along a UD-CFRP specimen length, extracted from a plate targeting 52.5 % FVF.

	Porosity (%)	FVF (%)
Mean	0.44	52.07
St. Dev.	0.13	4.03
C.o.V. (%)	29.54	7.74

4.4. Mechanical test methodology

The UD-CFRP and UD-BFRP plates were prepared and cut into specimens according to the mechanical test standards used in this study. For UD-CFRP, tensile tests were performed in the longitudinal direction (i.e. 0° direction) according to BS EN ISO 527-5 [74]. 10 specimens were tested for each of the four FVF sub-groups. For UD-BFRP, 0° & 90° tensile tests, 0° & 90° flexural tests, and 0° compression tests were performed according to BS EN ISO 527-5, BS EN ISO 14125 [75], and ASTM D6641/D6641M-16E1 [76], respectively. In each type of test, 8 specimens were tested.

Additional 0° tensile tests (BS EN ISO 527-5) were carried out for aged specimens which had been immersed in water. For UD-CFRP, specimens were immersed at room temperature (approx. 21°C), 50°C, and 75°C for 100 days. For UD-BFRP (Basaltex only), specimens were immersed at room temperature (approx. 21°C) and 55°C for 60 days. The specimens were periodically weighed using a microbalance to determine the water uptake over the duration of immersion. Tensile tests were also performed periodically to determine the influence of water uptake on the tensile properties of the specimens. In each case, 10 specimens were tested. Tensile testing was carried out when the specimens were still wet.

Tensile tests were performed using an MTS Criterion® Model 45 (C45.305) with a 300 kN load cell. A crosshead speed of 2 mm/min was used for all tensile tests. In all tensile test cases, the test specimens were end tabbed with ±45° GRFP and clamped in hydraulic grips with a clamping pressure of approx. 100 bar. A speckle pattern was applied to the surface of each specimen and 2D strain was measured with digital image correlation (DIC).

Compression tests were performed using an MTS Criterion® Model 45 (C45.305) with a 300 kN load cell and a fixture specially designed by Wyoming Test Fixtures for this specific type of test. Specimens were clamped by applying a torque of 4 N m. A crosshead speed of 1.3 mm/min was used for testing. Again, DIC was used to measure strain for all compression tests.

Flexural testing was performed using an Instron 3369 Dual Column Tabletop Test System with a 50 kN load cell. A four point bend fixture was used with an outer span of 45 mm (Class III, Table 4 of BS EN ISO 14125). Testing was carried out with a crosshead speed of 2.15 mm/min. DIC was used to track the midspan deflection of the test specimens.

5. Results and discussion

5.1. Fibre volume fraction investigations of UD-CFRP

Figure 10(a) shows the influence of FVF on the tensile properties of the UD-CFRP. The general trend was that the tensile properties (tensile strength, σ_M, and tensile modulus, E) improved with increasing FVF before decreasing above 57.5%. In addition to the void content analysis presented in Section 4.3, these results suggested that excellent consolidation was achieved at 47.5% FVF and 52.5% FVF. While the mean tensile properties of the 57.5% FVF specimens were the highest of the four sub-groups, the standard deviation (SD) was also the highest for both σ_M and E. This suggested that some specimens were well consolidated while others were not, due to insufficient wet-out and, consequently, poor load transfer between fibres and matrix. At 62.5%, this latter effect worsened and the mean tensile properties decreased. This upper limit in FVF was in agreement with what has been demonstrated for VBO prepregs previously [77]. At higher FVFs, consolidation was limited by the pressure that can be applied i.e. VBO pressure is 1 atm max. In this regard, Gutowski et al. [78] showed that FVF asymptotically approaches a maximum as a fibre bed compresses and resists the applied pressure. In the context of this study, higher FVF could be achieved via pultrusion of the towpreg through a die [69]. Further investigation of this concept was outside the scope of current work, however, it may be explored in future work (see Section 7). Alternatively, it is likely that additional autoclave or heated press processing would be required to achieve better quality and reliability above 60% FVF.

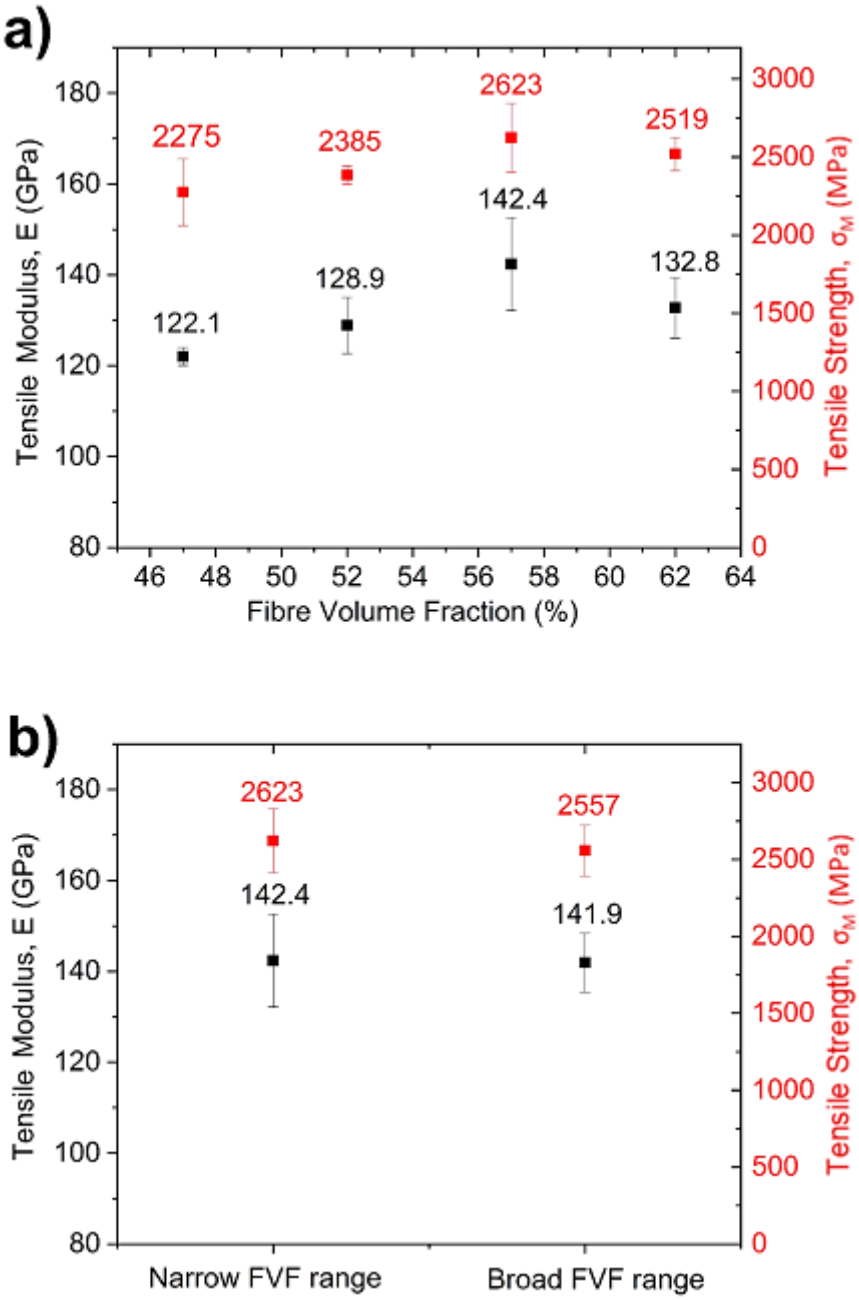

Figure 10: a) Influence of average FVF on 0° UD-CFRP mechanical properties.. b) Influence of strip FVF dispersion at 57.5 % FVF on 0° UD-CFRP mechanical properties.

To further study how mechanical properties may be affected by the FVF variation of towpreg, Figure 10(b) shows the results of two sets of specimens (both with an average FVF of 57.5%) which were manufactured using two different FVF ranges of towpreg. The original plate with 57.5% FVF contained strips of the same range (55% to 60%), called narrow FVF range. For the second plate, strips of various FVF were used, altering between high and low FVF layers of strips, but still overall reaching the same FVF as the first plate (i.e. broad FVF range). The results showed very similar values of σ_M and E. This suggested that the low viscosity of the powder-epoxy allowed for flow from resin-rich regions to resin-poor regions, leading to similar homogeneity for the two plates.

As previously mentioned, Mamalis et al. have studied the same powder-epoxy system with T700S-24K-50C fibres [33,35]. In their studies, plates were manufactured in a tensioning apparatus with powder manually dispersed onto the fibres. By using the same tensioning apparatus in this study, it was possible to directly compare the 0° tensile properties and determine whether the towpregging process had any adverse effect on the fibre properties. As shown in Table 3, the 0° tensile strength (σ_M) for 57.5% FVF specimens was almost identical to that which was reported by Mamalis et al. (for 59% FVF), while the 0° tensile modulus (E) was slightly higher. This confirms that the towpregging line does not have any significant adverse effect on the CF, such as fibre breakage.

Table 3 also shows the 0° tensile properties of other equivalent material systems of interest. As can be seen, the 57.5% FVF specimens were stronger and stiffer than the data reported by Toray for UD epoxy composites reinforced with T700s carbon fibres [56] while having a slightly lower FVF (57.5% compared to Toray's 60%). Comparatively, normalised data shows a substantial increase in both strength (+7.33%) and stiffness (+10.06%). This improvement was attributed to the improved fibre alignment achieved with the tensioning apparatus. This highlighted the technological potential for industrial manufacturing processes where carbon fibres are kept under tension, such as pultrusion, filament winding, and, to a lesser extent, ATP. For further comparison, Table 3 includes the 0° tensile properties of two flat-section pultruded CF/epoxy systems, both used for manufacturing turbine blade spars [79,80]. Both pultruded systems show higher FVF, but only the tensile modulus of Röchling EP-CFK (66% FVF) is higher than the 57.5% FVF UD-CRFP produced in this study. The lower 0° tensile strength can be attributed to a difference in fibre type and fibre quality e.g. the individual tensile fibre strength of T700S fibres [56] are markedly higher than Zoltek's PX35 fibres [81].

Table 3: Comparison of the 0° tensile properties for powder-epoxy UD-CFRP and equivalent material systems of interest.

	FVF (%)	σ_M(MPa)	SD (MPa)	E (GPa)	SD (GPa)
Towpreg line	47.5	2275.0	212.3	122.1	1.9
	52.5	2385.0	56.5	128.9	6.1
	57.5	2623.0	220.8	142.4	10.2
	62.5	2519.0	106.7	132.8	6.7
Mamalis et al. [33]	59.2	2650	-	134	-
Toray T700S [56]	60	2550	-	135	-
Gurit CF SparPreg [82]	56*	2234	-	140	-
Zoltek PX35 Pultruded Plate [83]	62	2350	-	140	-
Röchling EP-CFK [79]	66	2000	-	150	-

* Normalised to 56% in the technical data sheet

5.2. Comparison of UD-BFRP plates

Powder-based UD-BFRP plates were manufactured to compare Mafic and Basaltex basalt fibres. A FVF of 50% was targeted to ensure that homogeneous samples were processed. The results of the various

tests are plotted in Figure 11. Overall, the Basaltex fibre composites exhibited better mechanical properties than those with Mafic fibres. The mean strength of the Basaltex composite specimens was superior in 0° tension (+14%), 0° flexure (+24.3%) and 0° compression (27.4%), when compared to the Mafic composites. Basaltex composite specimens were also stiffer in 0° tension (+9.1%) and 0° flexure (+12.9%) but not in 0° compression (-5.5%). This important mismatch in properties is not unexpected as the basalt fibres are naturally sourced, and will display different properties as their chemical compositions depends on their extraction location [11].

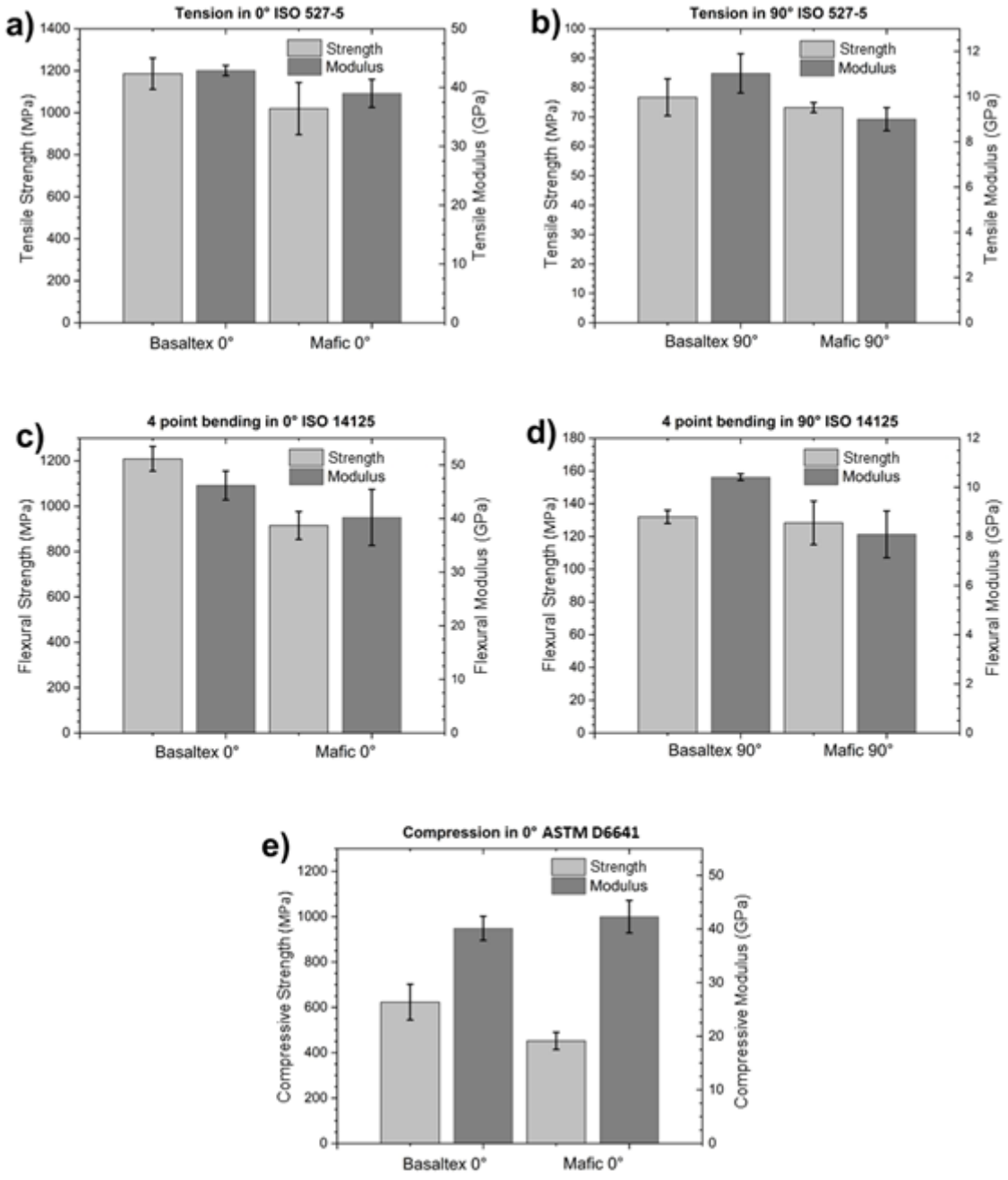

Figure 11: Mechanical properties of Basaltex and Mafic basalt towpreg based composites in tension (a & b), flexure(c & d) and compression (e).

The mechanical properties in the transverse direction allow a direct comparison of the interfacial properties, as the powder-epoxy is the same in both cases. Basaltex and Mafic BFRP displayed very similar strength in both 90° tension (+4.6% for Basaltex) and 90° flexure (+3% for Basaltex) configurations. As the tensile strength in transverse direction is largely matrix and fibre interface dominated, it was not surprising to obtain similar properties. Basaltex samples still exhibited much better transverse stiffness properties than Mafic specimens, doubling the difference already obtained longitudinally. It is likely that this is a result of a more effective fibre sizing.

For further comparative purposes, the results are reproduced in Table 4, Table 5, and Table 6 alongside mechanical properties for similar material systems. Direct comparison with other BFRP studies is difficult because much of the existing literature has focussed on the mechanical properties of bi-directional or multi-directional laminates [11,12]. Wang et al. [84] studied mechanical properties of UD-BFRP (epoxy matrix) in the 0° direction, comparing it to UD-GFRP in tension, compression, and flexure. They reported that the 0° tensile strength of the UD-BFRP (640 MPa) was much lower than UD-GFRP (1029 MPa), and attributed this to a variation in the tensile strength of individual fibre strands i.e. large variation in basalt fibre quality. Table 4 confirms that their values were much lower than the tensile strengths reported herein for Mafic fibres (37% lower) and Basaltex fibres (46% lower). Nevertheless, their 0° flexural strength was similar to the values for Mafic and Basaltex fibres, and notably, their 0° compressive strength was higher in both cases.

Table 4: Comparison of the tensile properties for powder-epoxy UD-BFRP and equivalent material systems of interest.

	FVF (%)	Test direction	σ_M(MPa)	SD (MPa)	E (GPa)	SD (GPa)
Mafic towpreg	50	0°	1020.0	124.0	39.0	2.4
		90°	73.2	1.7	9.0	0.5
Basaltex towpreg	50	0°	1186.0	74.3	42.9	0.9
		90°	76.7	6.3	11.0	0.9
Wang et al. [84] (UD-BFRP)	-	0°	640	-	40.8	-
Gurit GF Sparpreg* [82]	56**	0°	1225	-	48	-
	50	90°	42	-	12	-
Röchling EP-GZUV [79]	64	0°	1500	-	45-50	-

* Values for 1600 g/m^2

** Normalised to 56% in TDS

Davies and Verbouwe [15] investigated the mechanical properties of a stitched BFRP fabric with 357 g/m^2 in the 0° direction and 50 g/m^2 in the 90° direction (ratio of 7:1). Their quasi-UD BFRP fabric was made using Basaltex fibres sized for epoxy with alkosilane agent, which are believed to be very similar to the Basaltex fibres used in this study. The flexural strength reported in their work was 698 MPa, which is 42.3% lower than the value obtained in this study. Likely, this was due to the presence of

fibres in the transverse direction; typically used to stabilise the fabric while being laid up. Having less fibres aligned with the loading direction will reduce the strength in that direction, and will also increase the crimp of the BFRP, thus reducing the ultimate strength of composite materials [85].

Table 4, Table 5, and Table 6 also display values for commercially available material systems that are used for turbine blade spar caps; Gurit GF Sparpreg [82], a UD-GFRP prepreg system, and Röchling EP-GZUV [79], a UV-cured GF/epoxy pultruded section. Both UD-BFRP systems from this study compare favourably with the 0° tensile properties of the commercially available UD-GFRP (when factoring in the higher FVFs reported for the latter). Notably, the 90° tensile strengths were markedly higher for the powder-epoxy systems than for Gurit GF Sparpreg. These values were equal to the tensile strength of the neat powder-epoxy matrix (73.1 MPa [35]), which was atypical for conventional epoxy systems. Often some strength reductions are expected for transverse UD composite properties compared to neat matrix properties. These reductions are usually attributed to the presence of defects (such as voids), which form during composite processing, and aid crack initiation and propagation through the resin matrix. This is a particular issue for conventional epoxies, which are brittle, however, toughened epoxy systems have reported significantly better 90° tensile strengths: 90 MPa for Solvay's CYCOM® 5276-1 (G40-800 Tape) [86], 77 MPa for Hexcel's Hexply® 8552 UD CF prepreg [87], and 64 MPa for Hexcel's Hexply® M73/IM7 UD tape. In the latter case, the 90° tensile strength of the composite approached the tensile strength of the neat M73 epoxy i.e. 77 MPa). The improved performance of toughened epoxies may be attributed to their greater ability to resist crack growth compared to conventional systems. For the powder-epoxy in this study, it has been shown to have relatively ductile behaviour with exceptionally high mode I fracture toughness; between 1,100 and 1,900 J/m^2, depending on the fibre and sizing [35,88]. It should be noted that the ductile behaviour of the powder-epoxy is also evident in the tensile failure strain values for the 90° specimens: 0.92 ± 0.14%, which is high, compared to standard epoxy UD materials.

Table 5: Comparison of the flexural properties for powder-epoxy UD-BFRP and equivalent material systems of interest.

	FVF (%)	Test direction	σ_M(MPa)	SD (MPa)	E (GPa)	SD (GPa)
Mafic towpreg	50	0°	915.0	61.3	40.2	5.2
		90°	128.0	13.3	8.1	0.9
Basaltex towpreg	50	0°	1209.0	54.3	46.2	2.7
		90°	132.0	4.0	10.4	0.1
Wang et al. [84] (UD-BFRP)	-	0°	1115	-	43.7	-
Gurit GF Sparpreg* [82]	50	0°	1347	-	42	-
Röchling EP-GZUV [79]	64	0°	890-1020	-	35-45	-

* Values for 1200 g/m^2

The strong transverse performance of the UD-BFRP was confirmed by the 90° flexural properties which were similar to those reported by Mamalis et al. [33] for powder-epoxy UD-CFRP. 0° flexural properties were also similar to the UD-GFRP systems shown in Table 5. For 0° compressive properties (Table 5), however, the UD-BFRP again performed poorly compared to UD-GFRP. Failure was predominantly due to kinking of the fibres, despite the high degree of fibre alignment, which suggests that the ductile nature of the powder-epoxy played a role in the comparatively low 0° compressive properties.

Table 6: Comparison of the compressive properties for powder-epoxy UD-BFRP and equivalent material systems of interest.

	FVF (%)	Test direction	σ_M(MPa)	SD (MPa)	E (GPa)	SD (GPa)
Mafic towpreg	50	0°	452.0	38.0	42.3	3.0
Basaltex towpreg	50	0°	623.0	78.9	40.1	2.2
Wang et al. [84]	-	0°	836	-	-	-
Gurit GF Sparpreg* [82]	56**	0°	950	-	47	-

* Values for 1600 g/m^2

** Normalised to 56% in TDS

5.3. Hygrothermal aging

The results for 0° tensile testing of UD-CFRP (Figure 10 (a) and Table 3) show that the standard deviation was the lowest at 52.5% FVF; highlighting better reproducibility. As such, this FVF range was selected for a subsequent hygrothermal ageing study. In addition, Basaltex UD-BFRP was selected for the hygrothermal ageing study as it displayed better mechanical properties than Mafic UD-BFRP. UD-CFRP and UD-BFRP specimens were immersed in water as described in Section 4.4. In both cases, the temperature had an influence on the absorption rate and the water saturation level (see Figure 12).

As expected, rates of water absorption were highly temperature dependent. In the case of UD-CFRP, the specimens reached saturation within approx. 15 days of immersion at 75°C, but showed a high degree of scatter after that point with a potential loss of mass. Such a phenomena is not uncommon due to leaching of soluble components of the polymer matrix, which is exacerbated at higher temperatures [36]. At lower immersion temperatures, the UD-CFRP and UD-BFRP displayed similar characteristics, but differed in the quantity of water absorbed. Grogan et al. [36] reported similar differences in weight gain for powder-epoxy CFRP and GFRP specimens, despite the specimens having similar FVFs. Assuming that the water was predominantly absorbed by the resin matrix, they attributed this discrepancy to the difference in resin mass fraction (i.e. the resin mass fraction in the GFRP was lower due to the higher density of glass fibres (approx. 2520 kg/m^3) compared to carbon fibres (approx. 1800 kg/m^3)). They stopped short, however, of calculating the weight gain with respect to the resin mass fraction, W_r, using the simple equation,

$$W_r = \frac{W_c}{m_r} \quad (1)$$

Where W_c is the weight gain of the composite material, and m_r is the resin mass fraction of the composite material.

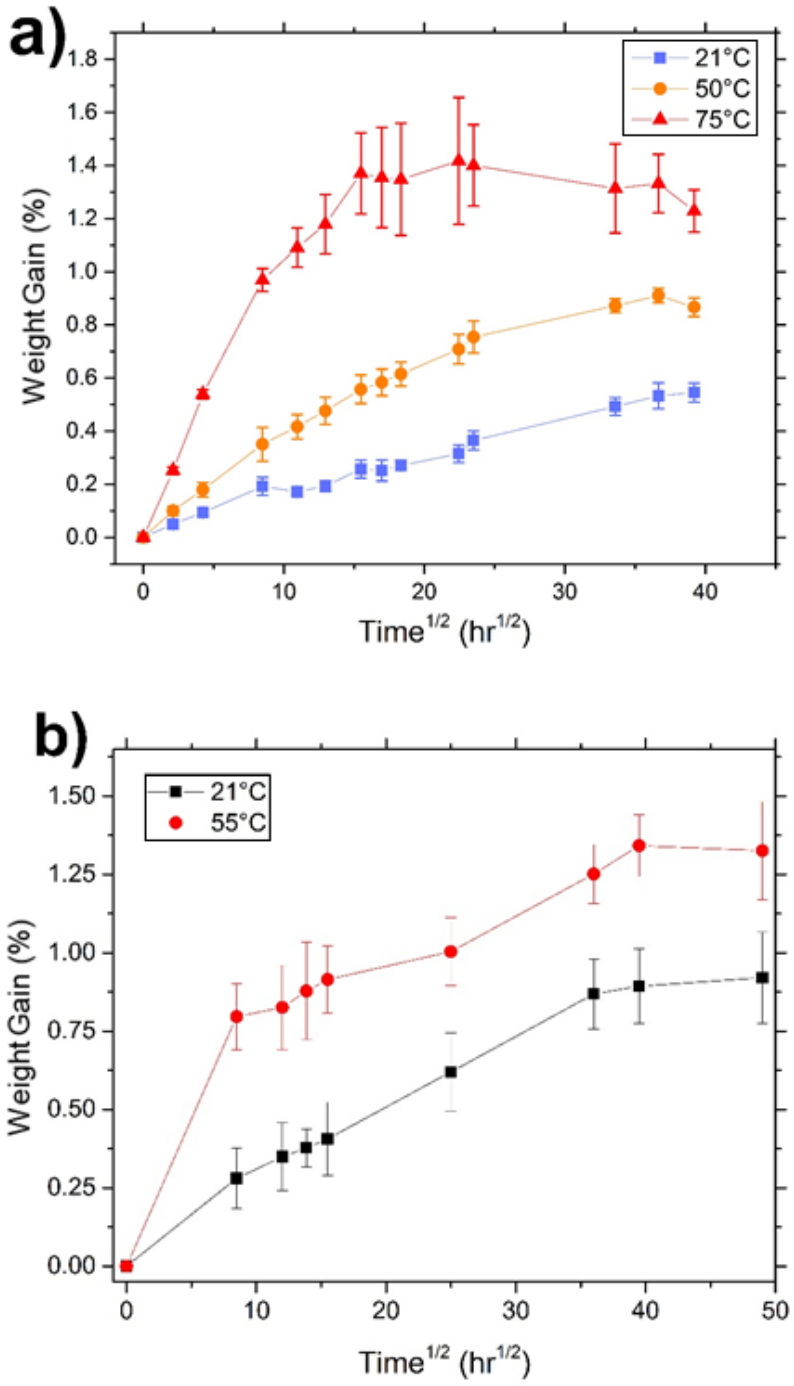

Figure 12: Composite weight gain (W_c) due to immersion of powder-epoxy based UD-CFRP (a) and UD-BFRP (b) against the square root of time at different temperatures.

Using Equation 1, it is possible to quantify the weight gain with respect to the resin mass fraction and compare it to the equivalent value for neat resin. For example, after 60 days at 50°C and ambient pressure, Grogan et al. [36] reported a weight gain of approx. 0.8% for GFRP (reported resin mass fraction of 33%), and approx. 1.0% for CFRP (reported resin mass fraction of 42%). Using Equation 1, this equates to 2.42% weight gain w.r.t to the resin mass fraction of the GFRP, and 2.38% weight gain w.r.t to the resin mass fraction of the CFRP. In comparison, under the same immersed conditions, they reported that the neat epoxy powder (density of 1220 kg/m^3) had a weight gain of approx. 2% with respect to its initial weight. This shows that both composites absorbed similar quantities of water, and both were slightly higher values than the weight gain of the neat resin. Applying the same calculation to the UD-CFRP in the current study (resin mass fraction of 38%), after 60 days at 50°C and ambient pressure, the specimens had a weight gain of approx. 2.26% w.r.t to the resin mass fraction of the CFRP. This shows excellent consistency between the two studies, and offers a simple, yet powerful method for analysing the influence of the polymer matrix on water absorption.

Although immersed ageing of the UD-BFRP was carried out at 55°C, it was considered that Equation 1 could provide some indication of how the composite performs in comparison to the UD-CFRP. As such, after 60 days at 55°C and ambient pressure, the UD-BFRP specimens were calculated to have increased in weight by approx. 4.14% with respect to the resin mass fraction (31.4% for a fibre density of 2670 kg/m^3 [58]). This was double the weight absorbed by the UD-CFRP in the same time span, but was consistent with the values reported by Davies and Verbouwe [15]. They performed water immersion studies (at 4°C, 25°C, 40°C, and 60°C) on quasi-UD GF/epoxy and BF/epoxy; Basaltex fibres were used in the latter case also. Interpolating between 40°C and 60°C at 60 days, their GFRP exhibited a weight gain of approx. 0.95%, while their BFRP exhibited a weight gain of approx. 1.15%. For their reported resin mass fractions of 36.2% (GFRP) and 33.5% (BFRP), this equates to weight gains, with respect to resin mass fraction, of 2.62% and 3.43%. Despite potential errors introduced by interpolation and approximation, these values are relatively consistent with both the values in this study (for BFRP) and the study by Grogan et al. [36] (for GFRP). For these studies, at least, this would suggest that water absorption in CFRP and GFRP was predominantly via the resin matrix, while there is some additional water absorption mechanism for the BFRP. As it is expected that the fibres would not absorb a significant amount of water (, this additional mechanism may be due to capillary action at the fibre-matrix interface, which can be damaged by swelling of the matrix [7]. Higher temperatures exacerbate this behaviour, which would allow more water ingress and increased saturation levels.

The effect of the additional water absorption was clearly visible in the aged mechanical performance of the UD-CFRP and UD-BFRP, as shown in Figure 13, which shows the 0° tensile strength and modulus plotted in relation to their weight gain due to water absorption. Based on the linear fits presented in Figure 13, UD-CFRP showed a reduction of 1.62% in tensile modulus and 8.79% tensile strength per 1 % weight gain, whereas basalt fibre samples displayed a greater dependency on water ingress, with reductions of 20.2% in tensile modulus and 24.5% in tensile strength per 1 % weight gain. Note that the individual data points are given in Table 7 and Table 8.

Davies and Verbouwe [15] tested their aged specimens in quasi-static flexure and cyclic flexure. The quasi-static tests, relevant to this study, showed comparatively less influence of water ageing on flexural modulus (approx. 5% reduction), but a very similar influence on flexural strength (approx. 24.6% reduction. They also noted that their GFRP were less sensitive to water ageing.

The increased water ageing of the BFRP was most likely coupled to the increased water absorption, and was also likely a result of damage accumulating at the fibre-matrix interface. This suggests that improved fibre sizings must be developed for BFRP to better retain its mechanical properties in immersed conditions.

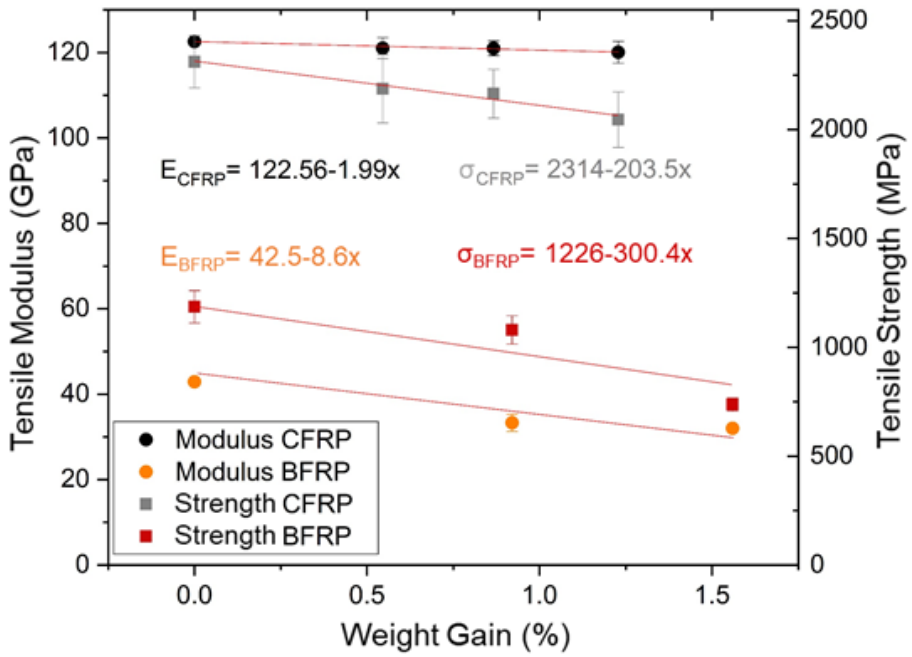

Figure 13: Mechanical properties of powder-epoxy based UD-CFRP and UD-BFRP in relation to their composite weight gain (W_c) due to water absorption.

Table 7: The influence of water ageing on the 0° tensile properties of UD-CFRP.

W_c (%)	σ_M(MPa)	SD (MPa)	E (GPa)	SD (GPa)
0.00	2311	120.2	122.6	0.5
0.55	2187	157.1	121.0	2.4
0.87	2164	112.1	121.0	1.7
1.23	2045	128.0	120.8	2.5

Table 8: The influence of water ageing on the 0° tensile properties of UD-BFRP.

W_c (%)	σ_M(MPa)	SD (MPa)	E (GPa)	SD (GPa)
0.00	1186	74.3	42.9	0.9
0.92	1080	64.9	33.3	2.0
1.56	737	29.9	32.0	0.5

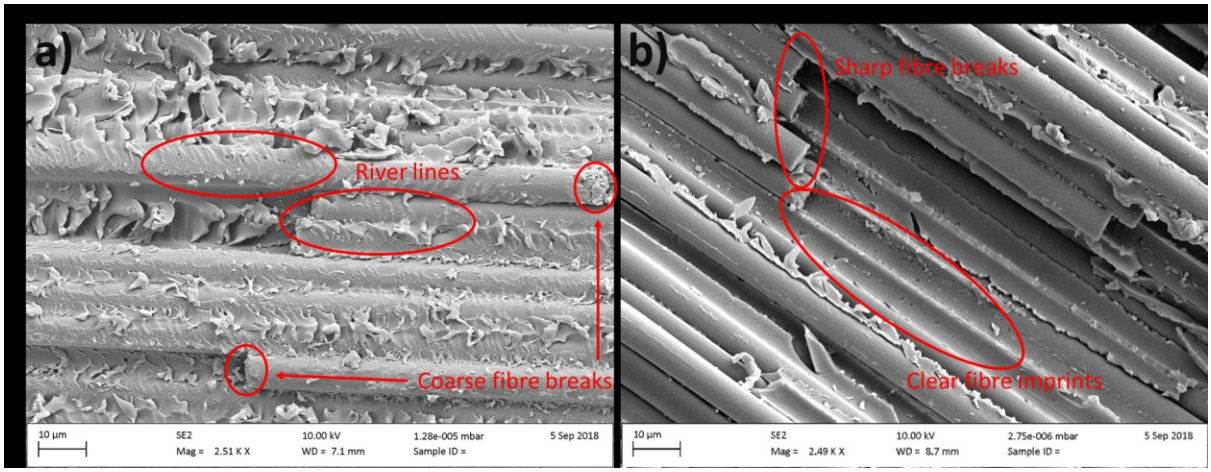

Figure 14: SEM fractographic photos of UD-CFRP epoxy samples a) dry and b) hygrothermally aged at 21˚C for 1600 hours.

The fracture comparison between dry and hygrothermally aged (21˚C) UD-CFRP samples highlights two different failure mechanism. The dry sample fracture reveals coarse fibre fractures with multiple fragmentation. One can also observe the presence of river lines on both the fibres and the fibre imprints. This fracture behavior is typical of good fibre/matrix interface cohesion, leading to a brittle and explosive failure. The presence of water in Figure 14(b) discloses a very different fracture behavior. Sharp, clean fibre breaks and clear fibre imprints are witness to a poorer energy transfer at the interface during breakage, when compared to the dry case of Figure 14 (a). The presence of water, plasticizing and swelling the resin, likely caused a poorer interfacial cohesion which resulted in a more ductile and progressive failure.

6. Conclusions

This study investigated a novel powder-epoxy towpregging line for manufacturing unidirectional carbon fibre reinforced polymers (UD-CFRP) and unidirectional basalt fibre reinforced polymers (UD-BFRP) as alternative material systems for ocean energy sub-structures such as wind and tidal turbine blade spars. One type of carbon fibre (CF) towpreg and two types of basalt fibre (BF) towpregs were produced; with powder-epoxy being used as the resin matrix in all cases.

Due to the processing characteristics of the powder-epoxy, it was possible to manufacture towpreg at 120°C without inducing any significant curing. Furthermore, once cooled below approx. 40°C (i.e. its glass transition temperature), it was possible to store the towpreg under ambient conditions with no risk of out-time effects.

Electrical joule heating was used during towpregging to sinter/melt the powder-epoxy onto the carbon fibres, while IR heating was used for basalt fibres. Both heating methods were successful in producing towpreg, however, it was found that electrical heating of CF towpreg resulted in a more homogeneous heating profile.

Electrostatic spraying was found to be an efficient method of powder deposition, however, a consistent deposition rate and stable line tension were found to be important for maintaining a uniform towpreg fibre volume fraction (FVF). Tensile tests (0° direction) on UD-CFRP specimens showed that strength and modulus increased with FVF up to 57.5%, but then reduced due to insufficient laminate processing pressure (i.e. vacuum-bag-only), resulting in poor consolidation at higher FVFs. It was also shown that the FVF range of CF/powder-epoxy towpreg had a negligible effect

on the 0° tensile properties as long as the mean FVF was at the required level. This was attributed to the low viscosity of the powder-epoxy, which allowed it to flow from resin-rich regions to resin-poor regions.

In all cases, test laminates were manufactured with a fibre tensioning apparatus, which improved fibre alignment and straightness, thereby improving the mechanical properties of the unidirectional composite laminates. By comparing directly to the literature, it was possible to show that the towpregging process had no adverse effect on the 0° tensile properties of the composite. Moreover, comparison with commercially available UD-CFRP material systems showed that similar or better 0° tensile properties were achievable with the CF towpreg.

For the two types of basalt fibre investigated, UD-BFRP manufactured with Basaltex fibres generally outperformed UD-BFRP manufactured with Mafic fibres in a series of mechanical tests; 0° & 90° tension, 0° & 90° flexure, and 0° compression. This confirmed that there was some variation between basalt fibre suppliers, however, similar variations might be expected between glass fibre suppliers or carbon fibre suppliers (e.g. Toray T700S compared to Zoltek PX35). Comparing to UD-BFRP from the literature and commercially available UD-GRFP, the two sets of UD-BFRP performed well in tension and flexure, with notably high 90° properties similar to the properties of the neat powder-epoxy. Despite this, both sets underperformed in 0° compression tests. The high 90° properties and low 0° compression properties are thought to be related to the ductility and toughness of the powder-epoxy.

Finally, a hygrothermal ageing study of UD-CFRP (52.5% FVF) and UD-BFRP (Basaltex, 50% FVF) showed that both composites absorbed water and aged as a result. For UD-CFRP, the weight gain (w.r.t to resin mass fraction) due to water uptake was similar to the literature for neat powder-epoxy. For UD-BFRP, however, the weight gain almost doubled (with respect to resin mass fraction) for similar ageing conditions to the CFRP. Further analysis of values reported in the literature, confirmed this trend for UD-CFRP and UD-BFRP. This suggested that there was some additional mechanism for water uptake in the UD-BFRP specimens other than absorption into the resin matrix; potentially capillary action due to damage at the fibre-matrix interface. This hypothesis was supported by a greater reduction in 0° tensile properties for UD-BFRP than UD-CFRP after immersed ageing. Similar trends were noted in the literature for UD-GFRP and UD-BFRP.

Overall, this study showed that the pilot towpregging line has potential for upscaling to produce UD materials for the ocean energy industry. In particular, the UD-CFRP produced in this study performed well against commercially available material systems and in immersed conditions. The results for UD-BFRP show an increasing potential for commercial use, but further development is still required to compete with GFRP or CFRP, particularly in area of immersed performance.

7. Future work

This study covered a broad range of themes; from material development and production, to mechanical testing and hygrothermal ageing. As such, exploring many aspects in detail were outside the current scope of work. Nevertheless, the results of the study open numerous possibilities for future work, some of which are presented here.

Firstly, this technology requires further automation before reaching an acceptable industrial level of reliability. Better process control and a deeper understanding of how each process parameter influences towpreg production can be achieved via process monitoring and process modelling. In this regard, key processes are tow tensioning, electrostatic deposition, heating, and consolidation. With

further development, data from tension meters, IR sensors, solid particle concentration sensors, and optical sensors could be logged in real time, and combined with process modelling to form a closed loop system which can be optimised and self-regulate.

The ability to produce high quality powder-epoxy towpreg would open numerous possibilities in terms of application due to its latent curing characteristics. Future projects will consider application of the towpreg in subsequent manufacturing processes. Towpreg could be used 'as-is' for filament winding, subsequently reprocessed into tape for ATP, or pultruded into net sections which can later be reformed. This latter example is significant in the context of the current work, which is aimed at developing alternative, low-cost materials for wind and tidal energy.

Acknowledgements

The authors would like to thank the European Commission for the financial support of the MARINCOMP and POWDERBLADE projects (FP7 IAPP ID: 612531 and Horizon 2020 ID: 730747 respectively), which made this study possible. The authors would also like to thank industrial supporters Freilacke, Mafic, Basaltex and Toray for supplying the material and details required for this study.

References

[1] Internation Energy Agency. Data and statistics 2020. https://www.iea.org/data-and-statistics?country=WORLD&fuel=Energy supply&indicator=Electricity generation by source (accessed June 1, 2020).

[2] WWEA. Wind Power Capacity reaches 546 GW, 60 GW added in 2017 2018. https://wwindea.org/blog/2018/02/12/2017-statistics/ (accessed June 1, 2020).

[3] Segura E, Morales R, Somolinos JA, López A. Techno-economic challenges of tidal energy conversion systems: Current status and trends. Renew Sustain Energy Rev 2017;77:536–50. https://doi.org/10.1016/j.rser.2017.04.054.

[4] Hollaway LC. 10 – High performance fibre-reinforced composites for sustainable energy applications. High Perform. Text. their Appl., Woodhead Publishing; 2014, p. 366–417. https://doi.org/https://doi.org/10.1533/9780857099075.366.

[5] Harper P, Hallett S, Fleming A, Dawson M. 9 – Advanced fibre-reinforced composites for marine renewable energy devices. Mar. Appl. Adv. Fibre-Reinforced Compos., Woodhead Publishing; 2016, p. 217–32. https://doi.org/https://doi.org/10.1016/B978-1-78242-250-1.00009-0.

[6] Nijssen R, de Winkel GD. 5 - Developments in materials for offshore wind turbine blades. Offshore Wind Farms, Woodhead Publishing; 2016, p. 85–104. https://doi.org/https://doi.org/10.1016/B978-0-08-100779-2.00005-2.

[7] Davies P, Rajapakse YDS. Durability of Composites in a Marine Environment. 1st ed. Springer Netherlands; 2014. https://doi.org/https://doi.org/10.1007/978-94-007-7417-9.

[8] Davies P, Rajapakse YDS. Durability of Composites in a Marine Environment 2. 2018. https://doi.org/10.1007/978-3-319-65145-3_13.

[9] Ross A. Basalt Fibers: Alternative to Glass ? Compos World 2006.

https://www.compositesworld.com/articles/basalt-fibers-alternative-to-glass (accessed June 16, 2020).

[10] Mason K. The still-promised potential of basalt ber composites. Compos World 2020. https://www.compositesworld.com/articles/the-still-promised-potential-of-basalt-fiber-composites (accessed June 16, 2020).

[11] Fiore V, Scalici T, Di Bella G, Valenza A. A review on basalt fibre and its composites. Compos Part B Eng 2015;74:74–94. https://doi.org/10.1016/j.compositesb.2014.12.034.

[12] Dhand V, Mittal G, Rhee KY, Park SJ, Hui D. A short review on basalt fiber reinforced polymer composites. Compos Part B Eng 2015;73:166–80. https://doi.org/10.1016/j.compositesb.2014.12.011.

[13] Wei B, Cao H, Song S. Degradation of basalt fibre and glass fibre/epoxy resin composites in seawater. Corros Sci 2011;53:426–31. https://doi.org/10.1016/j.corsci.2010.09.053.

[14] Fiore V, Di Bella G, Valenza a. Glass–basalt/epoxy hybrid composites for marine applications. Mater Des 2011;32:2091–9. https://doi.org/10.1016/j.matdes.2010.11.043.

[15] Davies P, Verbouwe W. Evaluation of Basalt Fibre Composites for Marine Applications. Appl Compos Mater 2018;25:299–308. https://doi.org/10.1007/s10443-017-9619-3.

[16] Jaksic V, Wallace F, Ó Brádaigh CM. Upscaling of Tidal Turbine Blades: Glass or Carbon Fibre Reinforced Polymers? Proc. Twelfth Eur. Wave Tidal Energy Conf., 2017.

[17] Pappa EJ, Murray JJ, Walls M, Alam P, Flanagan T, Doyle A, et al. Fatigue life analysis of hybrid E-glass/carbon fibre powder epoxy materials for wind turbine blades. ECCM 2018 - 18th Eur. Conf. Compos. Mater., 2018, p. 24–8.

[18] Murray RE, Swan D, Snowberg D, Berry D, Beach R, Rooney S. Manufacturing a 9-meter thermoplastic composite wind turbine blade. 32nd Tech. Conf. Am. Soc. Compos. 2017, vol. 1, 2017, p. 29–43. https://doi.org/10.12783/asc2017/15166.

[19] Bortolotti P. Carbon glass hybrid materials for wind turbine rotor blades. TU Delft, 2012.

[20] Ennis B, Kelley C, Naughton B, Norris R, Das S, Lee D, et al. Optimized Carbon Fiber Composites in Wind Turbine Blade Design. 2019.

[21] Swolfs Y. Perspective for fibre-hybrid composites in wind energy applications. Materials (Basel) 2017;10. https://doi.org/10.3390/ma10111281.

[22] Nijssen RPL, Brøndsted P. Fatigue as a design driver for composite wind turbine blades. 2013. https://doi.org/10.1533/9780857097286.2.175.

[23] Fagan EM, Wallace F, Jiang Y, Kazemi A, Goggins J. Design and testing of a full-scale 2 MW tidal turbine blade. Proc. 13th Eur. Wave Tidal Energy Conf., vol. 33, Naples: 2019.

[24] Sutcliffe MPF, Lemanski SL, Scott AE. Measurement of fibre waviness in industrial composite components. Compos Sci Technol 2012;72:2016–23. https://doi.org/10.1016/j.compscitech.2012.09.001.

[25] Wieland B, Ropte S. Process Modeling of Composite Materials for Wind-Turbine Rotor Blades: Experiments and Numerical Modeling. Materials (Basel) 2017;10:1157–69. https://doi.org/https://doi.org/10.3390/ma10101157.

[26] Kim D, Centea T, Nutt SR. Modelling and monitoring of out-time and moisture absorption effects on cure kinetics and viscosity for an out-of-autoclave (OoA) prepreg. Compos Sci

Technol 2017;138:201–8.
https://doi.org/https://doi.org/10.1016/J.COMPSCITECH.2016.11.023.

[27] Radanitsch J. Multi-layered Carbon Stacks for Large Wind Turbine Blades. Proc. CAMX 2014, Orlando, FL, USA: 2014.

[28] Cheney M. C., Migliore P. G. Feasibility Study of Pultruded Blades for Wind Turbine Rotors. Wind Eng 1999;23:145–58.

[29] O'Leary K, Pakrashi V, Kelliher D. Optimization of composite material tower for offshore wind turbine structures. Renew Energy 2019;140:928–42.
https://doi.org/10.1016/j.renene.2019.03.101.

[30] Maguire JM, Nayak K, Ó Brádaigh CM. Characterisation of epoxy powders for processing thick-section composite structures. Mater Des 2018;139:112–21.
https://doi.org/10.1016/J.MATDES.2017.10.068.

[31] Maguire JM, Simacek P, Advani SG, Ó Brádaigh CM. Novel epoxy powder for manufacturing thick-section composite parts under vacuum-bag-only conditions. Part I: Through-thickness process modelling. Compos Part A Appl Sci Manuf 2020;136.
https://doi.org/https://doi.org/10.1016/j.compositesa.2020.105969.

[32] Maguire JM, Nayak K, Ó Brádaigh CM. Novel epoxy powder for manufacturing thick-section composite parts under vacuum-bag-only conditions. Part II: Experimental validation and process investigations. Compos Part A Appl Sci Manuf 2020;136.
https://doi.org/https://doi.org/10.1016/j.compositesa.2020.105970.

[33] Mamalis D, Flanagan T, Ó Brádaigh CM. Effect of fibre straightness and sizing in carbon fibre reinforced powder epoxy composites. Compos Part A Appl Sci Manuf 2018;110:93–105.
https://doi.org/https://doi.org/10.1016/j.compositesa.2018.04.013.

[34] Murray JJ, Pappa EJ, Mamalis D, Breathnach G, Doyle A, Flanagan T, et al. Characterisation of carbon fibre reinforced powder epoxy composites for wind energy blades. Proc. 18th Eur. Conf. Compos. Mater., Athens, Greece: 2018.

[35] Mamalis D, Murray JJ, McClements J, Tsikritsis D, Koutsos V, McCarthy ED, et al. Novel carbon-fibre powder-epoxy composites: Interface phenomena and interlaminar fracture behaviour. Compos Part B Eng 2019:107012.
https://doi.org/10.1016/J.COMPOSITESB.2019.107012.

[36] Grogan D, Flanagan M, Walls M, Leen S, Doyle A, Harrison N, et al. Influence of microstructural defects and hydrostatic pressure on water absorption in composite materials for tidal energy. J Compos Mater 2018;52:2899–917.
https://doi.org/https://doi.org/10.1177/0021998318755428.

[37] Finnegan W, Glennon C, Kelly G, Maguire J, Flanagan M. Manufacture of High Performance Tidal Turbine Blades using Composite Materials. 13th Eur. Wave Tidal Energy Conf., Naples: 2019.

[38] Gherlone L, Rossini T, Stula V. Powder coatings and differential scanning calorimetry: the perfect fit. Prog Org Coatings 1998;34:57–63. https://doi.org/https://doi.org/10.1016/S0300-9440(98)00039-3.

[39] Sharma S, Luzinov I. Ultrasonic curing of one-part epoxy system. J Compos Mater 2011;45:2217–24. https://doi.org/https://doi.org/10.1177/0021998311401075.

[40] Ó Brádaigh CM, Doyle A, Doyle D, Feerick PJ. Electrically-Heated Ceramic Composite Tooling

for Out-of-Autoclave Manufacturing of Large Composite Structures. SAMPE J 2011;47.

[41] Edie D., Lickfield GC, Allen LE, McCollum JR. Thermoplastic Coating of Carbon Fibres. Hampton, VA, USA: 1989.

[42] Bayha TD, Osborne PP, Thrasher TP, Hartness JT, Johnston NJ, Marchello JM, et al. Processing, Properties and Applications of Composites Using Powder-Coated Epoxy Towpreg Technology. Proc. NASA's 4th Adv. Compos. Technol. Conf., Salt Lake City, Utah: 1993.

[43] Ramasamy A, Wang Y, Muzzy J. Braided thermoplastic composites from powder-coated towpregs. Part I: Towpreg characterization. Polym Compos 1996;17:497–504. https://doi.org/https://doi.org/10.1002/pc.10639.

[44] Allred RE, Wesson SP, Babow DA. Powder Impregnation Studies for High Temperature Towpregs. SAMPE J 2004;40:40–8.

[45] Nunes JP, van Hattum FWJ, Bernardo CA, Brito AM, Pouzada AS, Silva JF, et al. Chapter 11 Production of Thermoplastic Towpregs and Towpreg- Based Composites. Polym. Compos. from Nano- to Macroscale, 2005, p. 189–213.

[46] Stone KR, Springer JJ. Advanced Composites Technology Case Study at NASA Langley Research Center. 1995.

[47] Padaki S, Drzal LT. A Consolidation Model for Polymer Powder Impregnated Tapes. J Compos Mater 1997;31:2202-2227[1] S. Padaki, L.T. Drzal, A Consolidatio. https://doi.org/10.1177/002199839703102105.

[48] Nunes JP, Silva JF, Novo PJ. Processing Thermoplastic Matrix Towpregs by Pultrusion. Adv Polym Technol 2013;32:E306–12. https://doi.org/10.1002/adv.21279.

[49] Robert C, Mamalis D, Alam P, Lafferty AD, Ó Cadhain C, Breathnach G, et al. Powder Epoxy Based UD-CFRP Manufacturing Routes For Turbine Blade Application. Proc. SAMPE Eur. Conf. '18, Southampton, UK: 2018.

[50] Robert C, Pecur T, McCarthy ED, Ó Brádaigh CM. Tidal turbine blade composites using basalt fibre. 22nd Int. Conf. Compos. Mater., Melbourne: 2019.

[51] Yang P, Varughese B, Muzzy JD. Flexible thermoset towpregs by electrostatic powder fusion coating. Proc. 36th Int. SAMPE Symp. Exhib., San Diego, USA: 1991.

[52] Nunes JP, Bernardo CA, Pouzada AS, Edie DD. Modeling of the consolidation of polycarbonate/carbon fiber towpregs. Polym Compos 1999;20:260–8. https://doi.org/10.1002/pc.10353.

[53] Flanagan MH, Doyle F, Fagan E, Goggins J, Leen SB, Doyle A, et al. Large Scale Structural Testing of Wind Turbine Blades Manufactured Using a One- Shot Out-Of-Autoclave Process. Proc Civ Eng Res Irel Conf 2016.

[54] Fagan EM, Flanagan M, Leen SB, Flanagan T, Doyle A, Goggins J. Physical experimental static testing and structural design optimisation for a composite wind turbine blade. Compos Struct 2017;164:90–103. https://doi.org/10.1016/J.COMPSTRUCT.2016.12.037.

[55] Damiano M, D'Ettore A. Structural design of a multi-megawatt wind turbine blade with ONE SHOT BLADE® Technology. J. Phys. Conf. Ser., vol. 1037, 2018. https://doi.org/10.1088/1742-6596/1037/4/042002.

[56] Toray Carbon Fibers America. T700S Data Sheet. 2019.

[57] Basaltex. Standard Portfolio - Rovings, Twisted Yarns & Chopped Fibers. 2000.

[58] Basaltex. Basaltex Basic Fibre Properties TDS. 2018.

[59] Mafic. Assembled Roving TDS. 2018.

[60] Padaki S, Drzal LT. A simulation study on the effects of particle size on the consolidation of polymer powder impregnated tapes. Compos Part A Appl Sci Manuf 1999;30:325–37. https://doi.org/https://doi.org/10.1016/S1359-835X(98)00115-8.

[61] Allred RE, Wesson SP, Gordon B. Real Time Process Control of Polymer Loading on Powder Towpreg. SAMPE Conf., Baltimore, USA: 2009.

[62] Garcia Nava R. Pilot Powder Impregnation Line for Carbon-Fibre Unidirectional Tape. The University of Edinburgh, 2016.

[63] Woolard DE, Ramani K. Electric field modeling for electrostatic powder coating of a continuous fiber bundle. J Electrostat 1995;35:373–87. https://doi.org/https://doi.org/10.1016/0304-3886(95)00029-A.

[64] Naskar AK, Edie DD. Consolidation of Reactive Ultem®Powder-coated Carbon Fiber Tow for Space Structure Composites by Resistive Heating. J Compos Mater 2006;40:1871–83. https://doi.org/10.1177/0021998306061300.

[65] Hayes SA, Lafferty AD, Altinkurt G, Wilson PR, Collinson M, Duchene P. Direct electrical cure of carbon fiber composites. Adv Manuf Polym Compos Sci 2015;1:112–9. https://doi.org/10.1179/2055035915Y.0000000001.

[66] Dugger JA, Hirt DE. PMR-15/carbon fiber composites produced from powder-coated towpreg. Polym Compos 1996;17:492–6. https://doi.org/10.1002/pc.10638.

[67] Parasnis NC, Ramani K, Borgaonkar HM. Ribbonizing of electrostatic powder spray impregnated thermoplastic tows by pultrusion. Compos Part A Appl Sci Manuf 1996;27:567–74. https://doi.org/10.1016/1359-835X(96)00017-6.

[68] Brown JH, Colton JS. A machine system for the rapid production of composite structures. Polym Compos 2000;21:124–33. https://doi.org/10.1002/pc.10171.

[69] Novo PJ, Silva JF, Nunes JP, Marques AT. Pultrusion of fibre reinforced thermoplastic pre-impregnated materials. Compos Part B Eng 2016;89:328–39. https://doi.org/https://doi.org/10.1016/j.compositesb.2015.12.026.

[70] Miller A, Wei C, Gibson AG. Manufacture of polyphenylene sulfide (PPS) matrix composites via the powder impregnation route. Compos Part A Appl Sci Manuf 1996;27:49–56. https://doi.org/https://doi.org/10.1016/1359-835X(95)00010-Y.

[71] Kratmann K, Sutcliffe M, Lilleheden L, Pyrz R, Thomsen O. A novel image analysis procedure for measuring fibre misalignment in unidirectional fibre composites. Compos Sci Technol 2009;69:228–38. https://doi.org/10.1016/j.compscitech.2008.10.020.

[72] Wang J, Potter KD, Etches J. Experimental investigation and characterisation techniques of compressive fatigue failure of composites with fibre waviness at ply drops. Compos Struct 2013;100:398–403. https://doi.org/10.1016/j.compstruct.2013.01.010.

[73] Mehdikhani M, Gorbatikh L, Verpoest I, Lomov S V. Voids in fiber-reinforced polymer composites: A review on their formation, characteristics, and effects on mechanical performance. J Compos Mater 2019;53:1579–669. https://doi.org/10.1177/0021998318772152.

[74] BS EN ISO 527-5. Plastics — Determination of tensile properties - Part 5: Test conditions for unidirectional fibre-reinforced plastic composites. 2009. https://doi.org/10.1016/j.fertnstert.2015.12.022.

[75] BS EN ISO 14125. Fibre-reinforced plastic composites — Determination of flexural properties. 1998.

[76] ASTM D6641/D6641M - 16E1. Standard Test Method for Compressive Properties of Polymer Matrix Composite Materials Using a Combined Loading Compression (CLC) Test Fixture. 2016.

[77] Centea T, Grunenfelder LK, Nutt SR. A review of out-of-autoclave prepregs – Material properties, process phenomena, and manufacturing considerations. Compos Part A Appl Sci Manuf 2015;70:132–54. https://doi.org/https://doi.org/10.1016/j.compositesa.2014.09.029.

[78] Gutowski TG, Cai Z, Bauer S, Boucher D, Kingery J, Wineman S. Consolidation Experiments for Laminate Composites. J Compos Mater 1987;21:650–69. https://doi.org/https://doi.org/10.1177/002199838702100705.

[79] Röchling. Pultruded profiles for spar caps 2020. https://www.roechling-industrial.com/uk/industries/renewable-energies/plastics-for-wind-energy/materials-for-wind-turbine-blades/spar-caps-for-wind-turbines (accessed June 1, 2020).

[80] Legault M. Wind blade spar caps: Pultruded to perfection? Compos World 2018.

[81] ZOLTEK. Technical Datasheet PX35 Continuous Tow. 2020.

[82] Gurit. Carbon & Glass SparPreg ™ Full General Datasheet. 2016.

[83] ZOLTEK. Technical Datasheet PX35 Pultruded Profiles. 2020.

[84] Wang M, Zhang Z, Li Y, Li M, Sun Z. Chemical durability and mechanical properties of alkali-proof basalt fiber and its reinforced epoxy composites. J Reinf Plast Compos 2008;27:393–407. https://doi.org/10.1177/0731684407084119.

[85] Potter K, Khan B, Wisnom M, Bell T, Stevens J. Variability, fibre waviness and misalignment in the determination of the properties of composite materials and structures. Compos Part A Appl Sci Manuf 2008;39:1343–54. https://doi.org/10.1016/j.compositesa.2008.04.016.

[86] Solvay. Cycom ® 5276-1 Technical Data Sheet. 2019.

[87] Hexcel. HexPly ® 8552 Product Data Sheet. 2020.

[88] Floreani C, Robert C, Alam P, Davies P, Ó Brádaigh CM. Characterization of mode I interlaminar properties of novel composites for tidal turbine blades. 13th Eur. Wave Tidal Energy Conf., Naples: 2019.